AGU PUBLICATIONS

Geophysical Research Letters

RESEARCH LETTER
10.1002/2017GL072519

**Key Points:**
- Historical biogeophysical effects are dominated by land use
- For future effects, warming background climate and natural biogeographic shifts are substantial
- Temperature response depends on forest fractions prior to deforestation, which differ across scenarios

**Supporting Information:**
- Supporting Information S1

**Correspondence to:**
J. Winckler,
johannes.winckler@mpimet.mpg.de

**Citation:**
Winckler, J., C. H. Reick, and J. Pongratz (2017), Why does the locally induced temperature response to land cover change differ across scenarios?, *Geophys. Res. Lett.*, *44*, 3833–3840, doi:10.1002/2017GL072519.

Received 4 JAN 2017
Accepted 28 MAR 2017
Accepted article online 3 APR 2017
Published online 24 APR 2017



# Why does the locally induced temperature response to land cover change differ across scenarios?

**J. Winckler[1,2], C. H. Reick[1], and J. Pongratz[1]**

[1]Max Planck Institute for Meteorology, Hamburg, Germany, [2]International Max Planck Research School on Earth System Modeling, Hamburg, Germany

**Abstract** Land cover change (LCC) affects temperature locally. The underlying biogeophysical effects are influenced not only by land use (location and extent) but also by natural biogeographic shifts and background climate. We examine the contributions of these three factors to surface temperature changes upon LCC and compare them across Coupled Model Intercomparison Project phase 5 (CMIP5) scenarios. To this end, we perform global deforestation simulations with an Earth system model to deduce locally induced changes in surface temperature for historical and projected forest cover changes. We find that the dominant factors differ between historical and future scenarios: the local temperature response is historically dominated by the factor land use change, but the two other factors become just as important in scenarios of future land use and climate. An additional factor contributing to differences across scenarios is the dependence on the extent of forests before LCC happens: For most locations, the temperature response is strongest when starting deforestation from low forest cover fractions.

## 1. Introduction

Land cover change (LCC), such as a conversion from forests to grasslands, perturbs the local surface energy and water balance. Historically, these biogeophysical effects have been found to cool global climate [e.g., *de Noblet-Ducoudrė et al.*, 2012; *Boisier et al.*, 2012]. For future LCC in the representative concentration pathway (RCP) scenarios, the simulated biogeophysical effects were found to be substantially weaker [*Brovkin et al.*, 2013a; *Boysen et al.*, 2014; *Davies-Barnard et al.*, 2015]. The overall sign of the future response depends of course on the type of LCC (deforestation or afforestation dominating [*Davies-Barnard et al.*, 2015]), but even scenarios with the same general direction of LCC, such as the deforestation scenarios of RCP2.6 and RCP8.5, differ in their climatic effects [*Brovkin et al.*, 2013a]. Several factors have been proposed that are responsible for differences in LCC effects across scenarios [e.g., *Brovkin et al.*, 2013a; *Zhang et al.*, 2014; *Pitman et al.*, 2011]. In this study, we explore three factors (see next paragraph) that are relevant for the locally induced effects in past and future scenarios, and we compare their relative importance. We focus our analysis on the locally induced changes in surface temperature [e.g., *Kumar et al.*, 2013; *Malyshev et al.*, 2015; *Winckler et al.*, 2017]. Additionally, LCC may affect climate by nonlocal effects, such as advection of local changes in air temperature and humidity to neighboring regions. However, these nonlocal effects are triggered locally, such that a better understanding of interscenario differences should begin at a local level. Furthermore, local temperature changes are directly relevant for local living conditions.

The relative importance of the following three factors is assessed in our study: First, past and future effects may differ because of differences in areal extent and geographical distribution of *land-use-induced land cover change (LULCC)* in the scenarios [*Brovkin et al.*, 2013a]. Second, the effects of LCC at a given location will be modified by a *warming background climate (WARM)*, which may lead to a reduction in snow cover and changing evapotranspiration [*Pitman et al.*, 2011]. While the change in background climate between preindustrial and present-day conditions did not influence the LCC effects substantially [*de Noblet-Ducoudrė et al.*, 2012], the influence of a warming background climate may be substantial in future scenarios. Third, any change in background climate might cause natural biogeographic shifts, which we refer to as *climate-induced land cover change (CILCC)*; for instance, due to global warming, the tree-line in boreal regions is shifting northward [*ACIA*, 2004], and effects of this tree-line shift might accelerate warming locally [e.g., *Zhang et al.*, 2014]. While the factors LULCC, CILCC, and WARM have been investigated individually in previous studies [e.g., *Brovkin et al.*, 2013a; *Zhang et al.*, 2014; *Pitman et al.*, 2011], our approach enables us to determine their relative

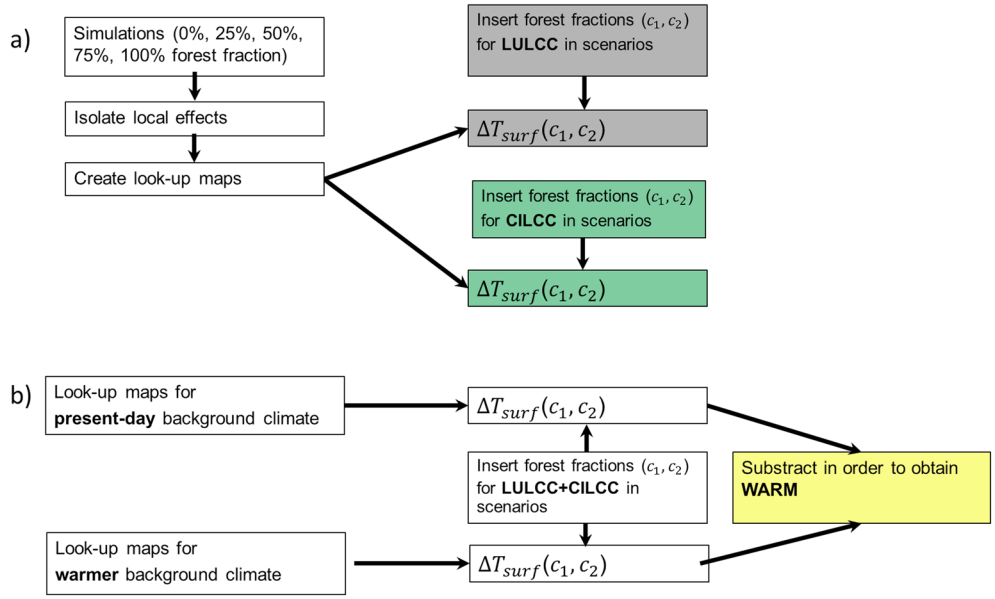


**Figure 1.** Conceptual diagram illustrating how changes in surface temperature are obtained for a given scenario of changes in forest fraction. See also section 2 for a methodological overview of the look-up approach. (a) We insert forest fraction for land-use (LULCC) or climate-induced land cover change (CILCC) into the look-up tables (see Figure 2) to obtain the corresponding temperature changes. The change in surface temperature $\Delta T_{surf}$ depends on the forest fractions at the beginning ($c_1$) and end ($c_2$) of the scenario. (b) We obtain the effect of warmer background climate (WARM) by comparing the effects in present-day background climate to the effects in a warmer background climate. To this end, we insert changes in LULCC + CILCC into two look-up tables that were obtained for different background climates. The colors correspond to the colors in Figure 3.

contribution within one set of simulations. This assessment of their relative contribution is essential to understand differences in the climate effects of LCC across scenarios.

In addition to the above factors, past and future scenarios differ in their initial forest cover fraction: In some areas that were partially deforested historically, deforestation or afforestation might take place in the future but starting from a lower initial forest cover fraction. Further, depending on the scenario, LCC happens in different regions showing more or less forest cover. These differences in initial forest cover fractions would not affect the results if, on a grid box level, climate responds linearly to deforestation. However, if climate responds nonlinearly to deforestation, this difference in initial forest cover fractions will contribute to the difference of the deforestation effects across the scenarios. Such a nonlinearity has been demonstrated in simulations by *Li et al.* [2016] for the total effects (locally induced plus remotely induced). We examine if this nonlinearity is also present for the locally induced changes in surface temperature and to what extent this nonlinearity contributes to the differences in the temperature response across LCC scenarios.

## 2. Methods: Look-Up Approach for the Locally Induced Changes in Surface Temperature

To infer locally induced changes in surface temperature from LCC—modeled here as a replacement of forests by grasslands—we proceed as follows (Figure 1a): We simulate changes in surface temperature following a stepwise reduction in the fraction that is covered with forest within each grid box ("forest fraction"). Then, we isolate the local effects as described by *Winckler et al.* [2017]. In each grid box, we interpolate the values that we obtained from the stepwise deforestation. The resulting curves then serve as look-up tables to infer temperature change from different LCC scenarios without the need for additional simulations: We insert the forest fractions at the start and the end of a scenario, and we obtain the change in surface temperature that is locally induced by this change in forest fraction (black arrow in Figure 2).

### 2.1. From Simulations to Look-Up Tables

First, we simulate changes in surface temperature following a reduction of forest fraction. We use the coupled land-atmosphere model ECHAM6/JSBACH [*Giorgetta et al.*, 2013; *Reick et al.*, 2013] at horizontal resolution T63

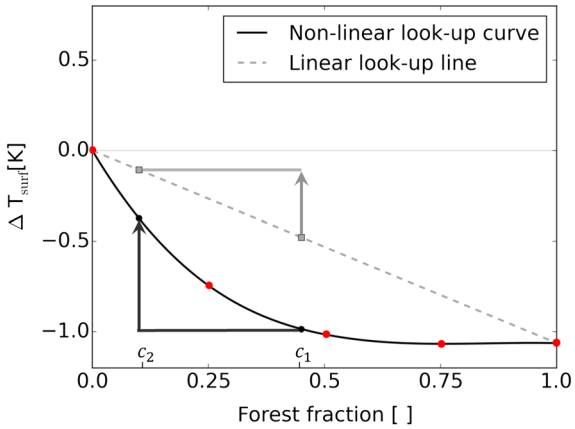


**Figure 2.** Illustration of the look-up approach for one selected grid box. Shown are the local effects from the five simulations with different forest fractions (red dots), the resulting interpolated look-up curve (black), and an artificial look-up line interpolating linearly between 100% and 0% forest cover (gray). The vertical axis denotes locally induced changes in surface temperature with respect to zero forest fraction. The arrows show the respective changes in surface temperature for a change in forest fraction from $c_1$ to $c_2$. In this example, the calculated change in surface temperature would be underestimated when using the linear look-up line.

(about 1.9°). In each experiment, we simulate 30 years after a 5 year spin-up. We impose present-day background climate: we prescribe sea surface temperatures (SSTs), sea ice, and $CO_2$ for the years 1976–2005 from the MPI-ESM CMIP5 (Coupled Model Intercomparison Project, phase 5) historical simulation [*Giorgetta et al.*, 2012a]. Following the approach of "sparse" deforestation described in *Winckler et al.* [2017], the conversion from forests to grasslands is performed in 1 out of 8 grid boxes arranged in a regular spatial pattern (see Figure 1 there). In the remaining boxes, present-day vegetation is left unchanged. This way, we ensure that background climate (the influence of which we investigate separately; see section 2.3) is not altered substantially by deforestation. To decrease the dependence of our results on the exact location of the deforestation grid boxes, we additionally simulate deforestation in 1 out of 8 grid boxes in a spatial pattern that is shifted by two grid boxes. For both the "shifted" and "unshifted" simulations, we then isolate the local effects by removing nonlocal effects and noise related to climate variability (for details see *Winckler et al.* [2017]). In the following, we consider the mean of the local effects from the "shifted" and "unshifted" simulations. Going beyond previously performed simulations [*Winckler et al.*, 2017], we isolate the local effects not only for complete deforestation within a grid box but deforest in steps of 25% starting from 100% forest cover in the vegetated part of each grid box. The bare land part of each grid box is left unchanged. We have then 5 forest fractions × 2 (shifted and unshifted) = 10 simulations.

For each land grid box, we compute 30 year means for each of the five experiments (illustrated by the red dots in Figure 2). We interpolate these means with a cubic spline. Using this curve $s()$ as a look-up table, we can convert a given change in forest fraction within the respective grid box (induced by LULCC, CILCC, or both) into a locally induced change in surface temperature (black arrow):

$$\Delta T_{\mathrm{surf}}(c_1, c_2) = s(c_2) - s(c_1), \tag{1}$$

where $c_1$ and $c_2$ denote the forest fractions within a grid box in the start and end year of the LCC scenario.

### 2.2. Forest Fraction Scenarios

We calculate the locally induced changes in surface temperature for various LCC scenarios: The historical scenario (between 1850 and 2005) and the future scenarios RCP2.6, RCP4.5, and RCP8.5 (between 2006 and 2099) of CMIP5. To determine the respective temperature response, we require the initial and final forest fractions (see equation (1)). These forest fractions are based on the land-use transitions data set by *Hurtt et al.* [2011], which is translated into geographical distributions of the plant functional types of MPI-ESM for CMIP5 as described in the paper by *Reick et al.* [2013] (see Figure S1 in the supporting information for LULCC-induced forest fraction changes in the respective scenarios). While we change the forest fractions within the vegetated part of a grid box, we keep this vegetated fraction fixed (see Text S1 and Figure S4).

For calculating forest fraction changes due to CILCC in the respective scenarios, we follow the approach by *Schneck et al.* [2015] and use the cover fractions from two existing simulations: The changes in forest fractions in the MPI-ESM simulations for CMIP5 [*Giorgetta et al.*, 2012a, 2012b, 2012c, 2012d] include both LULCC from the land-use transitions by *Hurtt et al.* [2011] and CILCC from JSBACH's dynamic vegetation module [*Reick et al.*, 2013] for the respective background climate. In a second data set, forest fraction changes are derived from the transitions by *Hurtt et al.* [2011], but the dynamic vegetation module is switched off [*Schneck et al.*, 2015]. We calculate CILCC as the difference in forest fraction change between these two data sets (see Figure S2 for

CILCC-induced forest fraction changes in the respective scenarios). The forest fraction changes can then be applied to the look-up tables to assess the impacts of LULCC and CILCC on surface temperature. In the case of a nonlinear response of surface temperature to deforestation, it matters whether LULCC or CILCC are applied first. However, in our study this is irrelevant, as LULCC and CILCC are affecting different regions, and thus the synergies between them are negligible (see Figure S3).

### 2.3. Determining the Influence of a Warmer Background Climate

In different background climates, a given change in land cover may affect surface temperature differently. While in reality background climate varies transiently, we consider the difference between the effects in two distinct background climates: present-day and the warmer RCP8.5 background climate. In addition to the look-up tables for present-day background climate (described in section 2.1), we create separate look-up tables for the warmer RCP8.5 background climate. For this, we repeat all 10 simulations described in section 2.1, but we prescribe SSTs, sea ice, and $CO_2$ from the years 2070–2099 from an MPI-ESM RCP8.5 simulation [*Giorgetta et al.*, 2012d]. Instead of RCP8.5, we could also assess the effect of the climate change projected under RCP2.6 or RCP4.5. However, for comparability across scenarios, we want to assess how one given change in background climate influences the results for the respective LCC scenarios. We choose the RCP8.5 forcing scenario because it exhibits the strongest warming of the RCP scenarios and thus can be seen as an upper bound for the relevance of background warming.

We calculate the influence of the warmer background climate as follows (see Figure 1b): The LCC effects are calculated separately for the look-up table corresponding to the warmer background climate $\tilde{s}()$ and the present-day background climate $s()$. Then, we define the influence of the warming background climate as the difference between these two results:

$$\Delta T_{\mathrm{surf}}^{\mathrm{WARM}}(c_1, c_2) = \left[\tilde{s}(c_2) - \tilde{s}(c_1)\right] - \left[s(c_2) - s(c_1)\right]. \tag{2}$$

Here $c_1$ and $c_2$ are the forest fractions within a grid box in the years 1850 and 2099. We choose to include LCC since 1850 (and not only LCC in the RCP scenarios starting in 2006) in the analysis of warming background climate for the following reasons: Background warming (mainly warming SSTs) is projected to occur only in the future. However, the resulting change of surface temperature within a land grid box is not only determined by LCC in the future but also by the forest fraction before the background warming. For instance, a given decrease in snow cover might cause warming in a fully forested grid box. However, if this grid box was deforested before the year 2005, this warming might be even more pronounced: The albedo in the grassland grid box (now without snow masking of trees) might respond stronger to the change in snow cover. Thus, the response of a grid box to post-2005 background warming also depends on pre-2005 LCC. Consequently, for calculating the effect of warming background climate, we also account for LCC prior to the year 2005. Since our LCC scenario starts in the year 1850, we do not account for LCC prior to the year 1850.

## 3. Causes of Differences in Temperature Response to LCC Across Scenarios

### 3.1. Land-Use-Induced and Climate-Induced Land Cover Change

When averaged over land, the locally induced changes in surface temperature of LULCC cause a cooling in the afforestation scenario RCP4.5, but warming in all other scenarios, which are the deforestation scenarios (Figure 3b; corresponding maps in Figure S1).

The temperature changes of CILCC are negligible for historical deforestation and induce a warming in all RCPs. As opposed to land-use-induced changes in forest cover, in every scenario there are both areas with forest gain and forest loss (Figure S2). Large parts of these climate-induced gains and losses of forest area compensate for each other and result in a relatively small temperature signal when averaged over the land surface. Note that CILCC in semiarid and arid regions may be overestimated because the vegetated fraction of the grid boxes there is overestimated by JSBACH [*Brovkin et al.*, 2013b]. However, this overestimation has only a small impact on our globally averaged results: Warming and cooling from forest fraction decrease and increase largely cancel each other out from these regions on a global scale. More important for the land-mean signal are a forest die-back in the Amazon (especially in RCP8.5), where forest has a cooling effect, and a northern shift of the tree line in the boreal regions (in all RCPs), where forest has a warming effect. While the likelihood of forest die-back in a warmer climate is still unclear [e.g., *Sitch et al.*, 2008; *Rammig et al.*, 2010], there is a broad consensus that the boreal tree line is about to shift northward as global warming proceeds [*ACIA*, 2004].

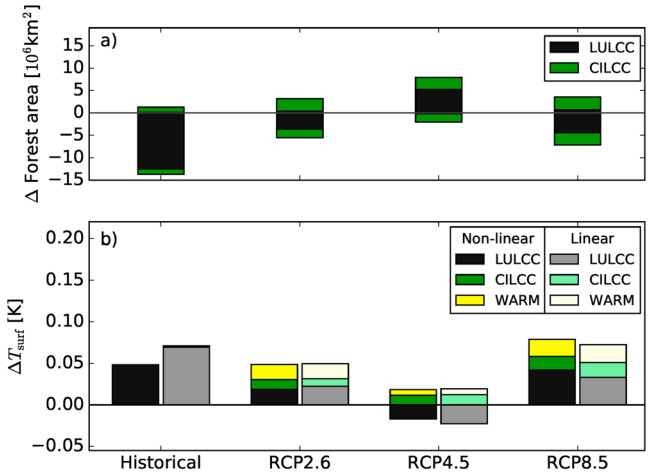


**Figure 3.** Comparison of LCC effects across scenarios. (a) Changes in global forest area. Within a scenario, there can be both areas of forest gain (positive values) and forest loss (negative values). (b) Contributions to local surface temperature changes from land-use-induced LCC, climate-induced LCC, and warming background climate. The vertical axis denotes surface temperature change averaged over land. For each scenario, the left bars account for the nonlinear surface temperature response, and the right bars assume a linear response to deforestation.

### 3.2. Influence of Changing Background Climate

In the warmer background climate, the surface warming induced locally by deforestation is stronger compared to the effects in present-day background climate. In present-day background climate, a conversion from 100% forests to 100% grasslands in an average grid box leads to a warming of 0.61 K, while the same effect in the warmer background climate is a warming of 0.75 K (see maps in Figure S5). In the temperate and boreal regions, these changes are associated with reduced snow cover fraction in the warmer background climate (not shown), in accordance with the study by *Pitman et al.* [2011]. Due to this reduced snow cover, deforestation leads to a smaller albedo increase, and thus, deforestation in the boreal regions becomes less cooling. Also, tropical deforestation in the warmer climate warms the surface more compared to deforestation in present-day climate. This additional warming results from stronger deforestation-induced decreases of turbulent heat fluxes in a warmer climate (not shown). Qualitatively, the change due to a warming background climate is in accordance with the study by *Armstrong et al.* [2016]: In their model, deforestation leads to a cooling, and in a warmer background climate this cooling effect decreases.

The change in background climate affects the results for the RCP scenarios: The effects of LCC in the warmer background climate are more warming compared to deforestation effects in present-day background climate (yellow bars in Figure 3b). For instance in RCP8.5, the influence of background warming on the LCC effects is 0.0204 K. This number consists of the contributions from historical LCC (0.0128 K) and LCC occurring between the years 2006 to 2099 (0.0076 K). Note that these two time spans are summarized in the yellow bars because we assign LCC in both time spans to the future scenario where background warming might occur. In contrast, the green and black bars only contain the contributions from LCC in the respective scenario.

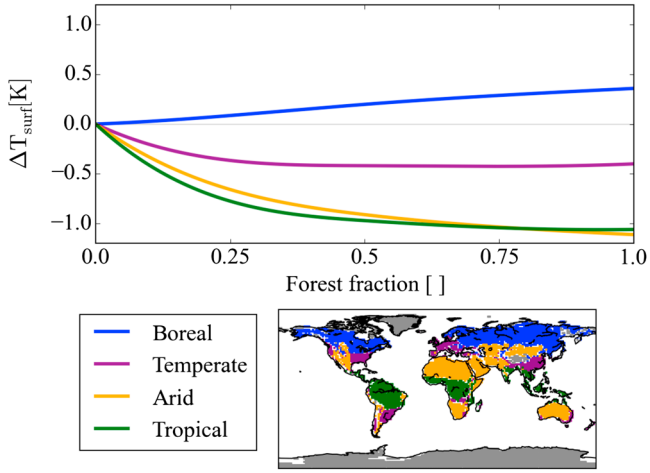


**Figure 4.** The nonlinearity differs across ecoregions. (top) Spatial averages of the already interpolated look-up maps for different ecoregions. The vertical axis denotes locally induced changes in surface temperature with respect to zero forest fraction. (bottom) Ecoregions that are used for averaging.

### 3.3. Influence of the Forest Fraction Prior to LCC

Here we assess whether surface temperature responds nonlinearly to the extent of deforestation within a grid box. Such a nonlinearity is relevant for the LCC scenarios: In case of a strong nonlinearity, the LCC effect depends on the forest fraction prior to deforestation. For instance in Figure 2, the change from $c_1$ to $c_2$ (black arrow) would have caused substantially less warming if the same extent of deforestation, $c_2 - c_1$, had started from a higher forest fraction. In contrast,

in case of a linear surface temperature response the deforestation effect would be independent of the forest fraction prior to LCC (grey arrow). The forest fraction prior to LCC varies across scenarios, and thus a nonlinearity, if existing, could contribute to differences in the LCC effects across scenarios.

Indeed, surface temperature responds nonlinearly to deforestation within most grid boxes (Figure 4). Deforestation is generally more efficient (that means deforestation causes more temperature change per unit forest fraction change) when starting from a low forest fraction. This nonlinearity is particularly strong in the temperate, arid, and tropical ecoregions, where surface temperature responds stronger to the last 25% than the first 75% of deforestation (Figure 4). The nonlinearity might arise from a nonlinear response of the turbulent heat fluxes to changes in surface roughness (not shown). Similar to this study, nonlinearities have been found in a previous simulation study by *Li et al.* [2016]. In their study, temperate and boreal changes in surface temperature were particularly strong when starting deforestation from high initial forest fractions. However, it is unclear if their nonlinearities were also present in the isolated locally induced effects or if their nonlinearities originated from changes in global circulation due to their approach of global deforestation. Our results show that nonlinearities are not only present in the total (local plus nonlocal) effects but can also be strong for the isolated locally induced changes in surface temperature. Thus, the deforestation impact depends on the forest fraction prior to LCC.

The nonlinearity contributes to the differences across the scenarios. To show this, we contrast our previous results (using the nonlinear look-up tables) by the results that would be obtained when ignoring the dependence on the forest fraction prior to LCC, and thus, calculating surface temperature changes using linear look-up tables (black curve versus grey line in Figure 2). The results are summarized in Figure 3b: For historical LULCC, the impact calculated using the nonlinear look-up tables is smaller than using the artificial linear look-up tables because the forest fraction prior to LCC in the historical scenario is relatively high (54% in the year 1850). The same is true for in RCP4.5, because LULCC largely consists of a reversal of historical deforestation. In the RCP2.6 scenario, the difference between the results for linear and nonlinear look-up tables becomes smaller, and in RCP8.5 the effect using the nonlinear look-up tables is even stronger compared to the results for the linear look-up tables. This is partly because the forest fractions prior to LCC are smaller than in the historical scenario (30% in the year 2005 for both RCP2.6 and RCP8.5).

## 4. Discussion

We use a look-up approach to calculate the locally induced changes in surface temperature. Compared to other methods for isolating the local effects [*Kumar et al.*, 2013; *Malyshev et al.*, 2015; *Lejeune et al.*, 2017], this approach has two advantages: First, the look-up approach allows us to assess the relative contribution of the three factors LULCC, CILCC, and WARM, without the need to perform computationally expensive simulations for each factor and scenario separately. Second, our approach allows us to assess the importance of the nonlinearity in the response and thus the dependence on the forest fraction prior to deforestation.

The look-up approach requires mutual independence of the LCC effects between different grid boxes. For the local effects in this study, this independence is given because the local effects within a grid box are largely independent of LCC elsewhere [*Winckler et al.*, 2017]. However, the nonlocal contributions from LCC are highly dependent on the spatial extent and distribution of LCC [e.g., *Swann et al.*, 2012; *Devaraju et al.*, 2015; *Winckler et al.*, 2017]. Thus, the look-up approach cannot be extended to include remotely triggered effects such as sea-ice-albedo feedbacks [e.g., *Swann et al.*, 2010; *Davies-Barnard et al.*, 2014].

The locally induced changes in surface temperature are relatively small when averaged over land but can be substantial on the local scale (Figures S1, S2, and S6). However, we display land average values in Figure 3 for the sake of comparability across factors and scenarios. Apparently, the averaging over all land areas partly obscures the fact that particularly the factors CILCC and WARM are warming locally in some regions, while they cool locally in others. Thus, their relative importance is larger than suggested by Figure 3b because the averaging artificially attenuates some of their effects (Figure S8).

There is a large spread in the response to LCC across the CMIP5 models, even for the isolated local effects [*Kumar et al.*, 2013; *Lejeune et al.*, 2017]. Also, the dependence on forest fraction prior to LCC and the three considered factors may differ across models, both concerning their relative importance and absolute quantification. Rather than giving an exact quantification, this study should be seen as illustrating that the relative contribution of the three factors can differ substantially across scenarios, up to a similar contribution of

CILCC and WARM as compared to LULCC for future scenarios. Thus, our study suggests that all three factors contribute substantially to the total climate effects of LCC.

While forest fractions prior to LCC have a relatively minor effect on the considered scenarios, they can be essential in other LCC scenarios. To illustrate this, we extend our assessment of realistic LULCC scenarios by an "idealized" deforestation scenario (see Text S2) similar to the experimental setup proposed for the Land-Use Model Intercomparison Project within CMIP6 [*Lawrence et al.*, 2016]. In such an idealized scenario, surface temperature responds particularly weakly because of the high forest fractions prior to deforestation (see Figures S1 and S7). These results highlight the need to be aware of the nonlinearity when comparing deforestation effects across scenarios. To evaluate whether the temperature response depends on the forest fraction prior to LCC in reality, further studies might assess the nonlinear behavior in observational data sets [e.g., *Li et al.*, 2015; *Alkama and Cescatti*, 2016].

## 5. Conclusions

Previous studies found that the climate effects of LCC differ across scenarios because of differences in the spatial extent and spatial distribution of land use [e.g., *Brovkin et al.*, 2013a]. Going beyond this, we identify two reasons why the locally induced changes in surface temperature differ across scenarios:

First, the relative contribution from land use, natural vegetation dynamics and warming background climate vary across scenarios. Historically, the locally induced changes in surface temperature have been dominated by land-use-induced land cover change (LULCC). In the scenarios for future development, the more indirect factors (warming background climate (WARM) and subsequent climate-induced land cover change (CILCC) might become of equal importance compared to land use. Background climate varies across scenarios, models, and ensemble members [e.g., *Sutton and Hawkins*, 2009], and for a given background climate, natural vegetation dynamics can differ substantially across dynamic global vegetation models [e.g., *Sitch et al.*, 2008]. Our results suggest that both uncertainties in the development of background climate and natural vegetation dynamics might add to the uncertainty of the LCC effects across models beyond the uncertainties in the implementation of LULCC and differences in the model parameterizations.

Second, forest fractions prior to deforestation vary between the historical scenario and future projections. These initial forest fractions influence the LCC effects, because surface temperature within a grid box responds nonlinearly to deforestation. These results have implications beyond this study: pre-LCC forest fractions differ not only across scenarios but also across models [e.g., *de Noblet-Ducoudré et al.*, 2012]. Thus, the nonlinearity might contribute to intermodel differences of LCC effects. If observational studies confirm our findings, the nonlinearity may also be relevant for local climate change mitigation.

**Acknowledgments**
We want to thank Daniela Kracher and one anonymous reviewer for detailed comments, which greatly helped to improve the manuscript. We thank Rainer Schneck for providing access to the forest fraction data from his simulations. Our simulations were performed at the German Climate Computing Center (DKRZ). This work was supported by the German Research Foundation's Emmy Noether Program (PO 1751/1-1). Primary data and scripts used in the analysis and other supporting information that may be useful in reproducing the author's work are archived by the Max Planck Institute for Meteorology and can be obtained by contacting publications@mpimet.mpg.de.

## References

ACIA (2004), Impacts of a warming Arctic: Arctic climate impact assessment, 1046 pp., Cambridge Univ. Press, doi:10.2277/0521617782.

Alkama, R., and A. Cescatti (2016), Biophysical climate impacts of recent changes in global forest cover, *Science*, *351*(6276), 600–604, doi:10.1126/science.aac8083.

Armstrong, E., P. Valdes, J. House, and J. Singarayer (2016), The role of $CO_2$ and dynamic vegetation on the impact of temperate land-use change in the HadCM3 coupled climate model, *Earth Interact.*, *20*(10), 1–10, doi:10.1175/EI-D-15-0036.1.

Boisier, J. P., N. de Noblet-Ducoudré, A. J. Pitman, F. T. Cruz, C. Delire, B. J. J. M. van den Hurk, M. K. van der Molen, C. Müller, and A. Voldoire (2012), Attributing the impacts of land-cover changes in temperate regions on surface temperature and heat fluxes to specific causes: Results from the first LUCID set of simulations, *J. Geophys. Res.*, *117*, D12116, doi:10.1029/2011JD017106.

Boysen, L. R., V. Brovkin, V. K. Arora, P. Cadule, N. de Noblet-Ducoudré, E. Kato, J. Pongratz, and V. Gayler (2014), Global and regional effects of land-use change on climate in 21st century simulations with interactive carbon cycle, *Earth Syst. Dyn.*, *5*, 309–319, doi:10.5194/esd-5-309-2014.

Brovkin, V., et al. (2013a), Effect of anthropogenic land-use and land-cover changes on climate and land carbon storage in CMIP5 projections for the twenty-first century, *J. Clim.*, *26*(18), 6859–6881, doi:10.1175/JCLI-D-12-00623.1.

Brovkin, V., L. Boysen, T. Raddatz, V. Gayler, A. Loew, and M. Claussen (2013b), Evaluation of vegetation cover and land-surface albedo in MPI-ESM CMIP5 simulations, *J. Adv. Model. Earth Syst.*, *5*, 48–57, doi:10.1029/2012MS000169.

Davies-Barnard, T., P. J. Valdes, J. S. Singarayer, F. M. Pacifico, and C. D. Jones (2014), Full effects of land use change in the representative concentration pathways, *Environ. Res. Lett.*, *9*(11), 114014, doi:10.1088/1748-9326/9/11/114014.

Davies-Barnard, T., P. J. Valdes, J. S. Singarayer, a. J. Wiltshire, and C. D. Jones (2015), Quantifying the relative importance of land cover change from climate and land-use in the representative concentration pathways, *Global Biogeochem. Cycles*, *29*, 842–853, doi:10.1002/2014GB004949.

de Noblet-Ducoudré, N., et al. (2012), Determining robust impacts of land-use-induced land cover changes on surface climate over North America and Eurasia: Results from the first set of LUCID experiments, *J. Clim.*, *25*(9), 3261–3281, doi:10.1175/JCLI-D-11-00338.1.

Devaraju, N., G. Bala, and A. Modak (2015), Effects of large-scale deforestation on precipitation in the monsoon regions: Remote versus local effects, *Proc. Natl. Acad. Sci. U.S.A.*, *112*(11), 3257–3262, doi:10.1073/pnas.1423439112.

Giorgetta, M., et al. (2012a), CMIP5 simulations of the Max Planck Institute for Meteorology (MPI-M) based on the MPI-ESM-LR model: The historical experiment, served by ESGF, WDCC at DKRZ, doi:10.1594/WDCC/CMIP5.MXELHI.
Giorgetta, M., et al. (2012b), CMIP5 simulations of the Max Planck Institute for meteorology (MPI-M) based on the MPI-ESM-LR model: The RCP26 experiment, served by ESGF, WDCC at DKRZ, doi:10.1594/WDCC/CMIP5.MXELR2.
Giorgetta, M., et al. (2012c), CMIP5 simulations of the Max Planck Institute for Meteorology (MPI-M) based on the MPI-ESM-LR model: The RCP45 experiment, served by ESGF, WDCC at DKRZ, doi:10.1594/WDCC/CMIP5.MXELR4.
Giorgetta, M., et al. (2012d), CMIP5 simulations of the Max Planck Institute for Meteorology (MPI-M) based on the MPI-ESM-LR model: The RCP85 experiment, served by ESGF, WDCC at DKRZ, doi:10.1594/WDCC/CMIP5.MXELR8.
Giorgetta, M. A., et al. (2013), The atmospheric general circulation model ECHAM6 — Model description, Tech. Rep., Max-Planck-Institute for Meteorology 135, Hamburg, Germany.
Hurtt, G. C., et al. (2011), Harmonization of land-use scenarios for the period 1500–2100: 600 years of global gridded annual land-use transitions, wood harvest, and resulting secondary lands, *Clim. Change*, *109*, 117–161, doi:10.1007/s10584-011-0153-2.
Kumar, S., P. A. Dirmeyer, V. Merwade, T. DelSole, J. M. Adams, and D. Niyogi (2013), Land use/cover change impacts in CMIP5 climate simulations: A new methodology and 21st century challenges, *J. Geophys. Res. Atmos.*, *118*, 6337–6353, doi:10.1002/jgrd.50463.
Lawrence, D. M., et al. (2016), The Land Use Model Intercomparison Project (LUMIP) contribution to CMIP6: Rationale and experimental design, *Geosci. Model Dev.*, *9*, 2973–2998, doi:10.5194/gmd-9-2973-2016.
Lejeune, Q., S. I. Seneviratne, and E. L. Davin (2017), Historical land-cover change impacts on climate: Comparative assessment of LUCID and CMIP5 multi-model experiments, *J. Clim.*, *30*(4), 1439–1459, doi:10.1175/JCLI-D-16-0213.1.
Li, Y., M. Zhao, S. Motesharrei, Q. Mu, E. Kalnay, and S. Li (2015), Local cooling and warming effects of forests based on satellite observations, *Nat. Commun.*, *6*, 6603, doi:10.1038/ncomms7603.
Li, Y., N. de Noblet-Ducoudrė, E. L. Davin, N. Zeng, S. Motesharrei, S. C. Li, and E. Kalnay (2016), The role of spatial scale and background climate in the latitudinal temperature response to deforestation, *Earth Syst. Dyn. Discuss.*, *7*, 167–181, doi:10.5194/esdd-6-1897-2015.
Malyshev, S., E. Shevliakova, R. J. Stouffer, and S. W. Pacala (2015), Contrasting local versus regional effects of land-use-change-induced heterogeneity on historical climate: Analysis with the GFDL Earth system model, *J. Clim.*, *28*(13), 5448–5469, doi:10.1175/JCLI-D-14-00586.1.
Pitman, A. J., F. B. Avila, G. Abramowitz, Y. P. Wang, S. J. Phipps, and N. de Noblet-Ducoudrė (2011), Importance of background climate in determining impact of land-cover change on regional climate, *Nat. Clim. Change*, *1*(9), 472–475, doi:10.1038/nclimate1294.
Rammig, A., T. Jupp, K. Thonicke, B. Tietjen, J. Heinke, S. Ostberg, W. Lucht, W. Cramer, and P. Cox (2010), Estimating the risk of Amazonian forest dieback, *New Phytol.*, *187*, 694–706, doi:10.1111/j.1469-8137.2010.03318.x.
Reick, C. H., T. Raddatz, V. Brovkin, and V. Gayler (2013), Representation of natural and anthropogenic land cover change in MPI-ESM, *J. Adv. Model. Earth Syst.*, *5*(3), 459–482, doi:10.1002/jame.20022.
Schneck, R., C. H. Reick, J. Pongratz, and V. Gayler (2015), The mutual importance of anthropogenically and climate-induced changes in global vegetation cover for future land carbon emissions in the MPI-ESM CMIP5 simulations, *Global Biogeochem. Cycles*, *29*, 1816–1829, doi:10.1002/2014GB004959.
Sitch, S., et al. (2008), Evaluation of the terrestrial carbon cycle, future plant geography and climate-carbon cycle feedbacks using five Dynamic Global Vegetation Models (DGVMs), *Global Change Biol.*, *14*(9), 2015–2039, doi:10.1111/j.1365-2486.2008.01626.x.
Sutton, R., and E. Hawkins (2009), The potential to narrow uncertainty in regional climate predictions, *Bull. Am. Meteorol. Soc.*, *90*(8), 1095–1107, doi:10.1175/2009BAMS2607.1.
Swann, A. L., I. Y. Fung, S. Levis, G. B. Bonan, and S. C. Doney (2010), Changes in Arctic vegetation amplify high-latitude warming through the greenhouse effect, *Proc. Natl. Acad. Sci. U.S.A.*, *107*(4), 1295–1300, doi:10.1073/pnas.0913846107.
Swann, A. L. S., I. Y. Fung, and J. C. H. Chiang (2012), Mid-latitude afforestation shifts general circulation and tropical precipitation., *Proc. Natl. Acad. Sci. U.S.A.*, *109*(3), 712–716, doi:10.1073/pnas.1116706108.
Winckler, J., C. H. Reick, and J. Pongratz (2017), Robust identification of local biogeopysical effects of land cover change in a global climate model, *J. Clim.*, *30*(3), 1159–1176, doi:10.1175/JCLI-D-16-0067.1.
Zhang, W., C. Jansson, P. A. Miller, B. Smith, and P. Samuelsson (2014), Biogeophysical feedbacks enhance the arctic terrestrial carbon sink in regional Earth system dynamics, *Biogeosciences*, *8*(034023), 1–10, doi:10.5194/bg-11-5503-2014.